

# NEUTRON FORM FACTOR: SUDAKOV SUPPRESSION AND INTRINSIC TRANSVERSE SIZE EFFECT

J. BOLZ, R. JAKOB and P. KROLL\*

*Fachbereich Physik*

*Universität Wuppertal*

*D-42097 Wuppertal, Germany*

M. BERGMANN and N. G. STEFANIS†

*Institut für Theoretische Physik II*

*Ruhr-Universität Bochum*

*D-44780 Bochum, Germany*

(November 6, 2018)

arXiv:hep-ph/9407250v2 11 Jul 1994

---

\*E-mail address: kroll@wpts0.physik.uni-wuppertal.de

†E-mail address: nicos@hadron.tp2.ruhr-uni-bochum.de

## Abstract

Two recently proposed concepts to improve the perturbative calculation of exclusive amplitudes, gluonic radiative corrections (Sudakov factor) and confinement size effects (intrinsic transverse momentum) are combined to study the neutron magnetic form factor in the space-like region. We find that nucleon distribution amplitudes modelled on the basis of current QCD sum rules indicate overlap with the existing data at the highest measured values of momentum transfer. However, sizeable higher-order perturbative corrections (K-factor) and/or higher-twist contributions cannot be excluded, although they may be weaker than in the proton case.

In a recent paper [1] we have studied the space-like proton form factor within a theoretical scheme proposed by Li and Sterman [2], which takes into account gluonic radiative corrections in the form of a Sudakov factor [3]. This scheme naturally generalizes the standard hard scattering picture (HSP) of Brodsky and Lepage [4]—commonly used to calculate exclusive reactions within perturbative QCD—by taking into account the transverse momentum of the partons.

A major point in our proton form-factor analysis was to show that proper treatment of the  $\alpha_s$ -singularities demands the imposition of an appropriate infrared (IR) cut-off to render the form-factor calculation both finite and insensitive to the inclusion of the soft region of phase space. This is in contrast to the pion case [2], where a “natural” IR cut-off appears in the form of the interquark separation. Considering in detail optional IR cut-off prescriptions [5–7], we found that maximum IR protection is provided by introducing as a common IR cut-off in the Sudakov (suppression) factor the maximum interquark separation (“MAX” prescription [1]). The underlying physical idea is the following: One expects that because of the color neutrality of a hadron, its quark distribution cannot be resolved by gluons with a wavelength much larger than a characteristic interquark separation scale  $\tilde{b}_l$ . Thus, gluons with wavelengths large compared to the (transverse) hadron size probe the hadron as a whole, i.e., in a color-singlet state and decouple. As a result, quarks in such configurations act coherently and therefore (soft) gluon radiation is dynamically inhibited.

The “MAX” prescription not only suffices to suppress the  $\alpha_s$ -singularities, but also preserves the finiteness of the integrand of the expression for the form factor, even when renormalization-group (RG) evolution of the wave function is included. An additional bonus of the “MAX” prescription is that the proton form factor saturates, i.e., becomes insensitive to the contributions from large transverse separations. Admittedly, little confidence is put in perturbative treatments of the large-distance region, so that saturation of the form factor at transverse distances as low as possible is a prerequisite for a self-consistent perturbative calculation.

In [1] we have pointed out that the recent numerical analysis by Li [5] of the proton

form factor has serious drawbacks: (i) The cancellation of the  $\alpha_s$ -singularities in the region  $\tilde{b}_l \Lambda_{\text{QCD}} \simeq 1$  ( $x_l$  fixed) is incomplete for different  $\tilde{b}_l$ , amounting to uncompensated singularities of the form

$$\sim \ln \left( \frac{1}{\tilde{b}_l \Lambda_{\text{QCD}}} \right)^\kappa. \quad (1)$$

(ii) There is no saturation, meaning that the main form-factor contributions are accumulated in the “forbidden” soft region.

A second element of our approach in [1] was the incorporation of the intrinsic transverse momentum in the proton wave function, following a previous work by two of us [8] on the pion form factor. The intrinsic transverse momentum reflects confinement-size effects [9] and improves the saturation behavior of the form factor. As a consequence of these effects (Sudakov factor and intrinsic transverse momentum), the self-consistent perturbative contribution to the proton form factor turns out to be reduced by at least a factor of two compared to the existing experimental data (see, e.g., [10,11]). This is true for a variety of nucleon distribution amplitudes (DA), recently determined by two of us [12,13] on the theoretical basis of QCD sum rules [14,15].

In the present work we extend this type of analysis to the neutron magnetic form factor. While in our previous work the focus was on the self-consistent implementation of the Sudakov factor and the proper identification and matching of the scales involved, the subject of the current effort will be on the phenomenological side. In particular, we consider observables involving the ratio of the neutron to the proton form factor  $G_M^n/G_M^p$ . It has been discussed in [16] (and previous references cited therein) and more recently in [17] that proposed model distribution amplitudes for the nucleon can be classified according to this ratio (an observable quantity) and the theoretical parameters  $B_4$  (projection coefficient on the corresponding eigenfunction of the nucleon evolution equation) and the “hybridity” angle  $\vartheta$ , as detailed in [13]. One of the crucial questions posed in the present work is whether the emerging pattern of solutions to the sum rules, found within the standard HSP [4,14] to constitute a smooth and finite “orbit” in the  $(B_4, -G_M^n/G_M^p)$  plane, pertains to the inclusion

of transverse-momentum contributions.

The starting point of our analysis is to consider the neutron magnetic form factor within the modified HSP:

$$G_M^n(Q^2) = \frac{16}{3} \int_0^1 [dx][dx'] \int \frac{d^2b_1}{(4\pi)^2} \frac{d^2b_2}{(4\pi)^2} \sum_{j=1}^2 \hat{T}_j(x, x', \vec{b}, Q, \mu) \hat{Y}_j^n(x, x', \vec{b}, \mu_F) e^{-S_j}, \quad (2)$$

with  $[dx] = dx_1 dx_2 dx_3 \delta(1 - \sum x_i)$ ;  $x_i$  being the momentum fractions carried by the valence quarks. The Fourier-transformed hard scattering amplitudes are given by

$$\hat{T}_1 = \frac{8}{3} C_F \alpha_s(t_{11}) \alpha_s(t_{12}) K_0 \left( \sqrt{(1-x_1)(1-x'_1)} Q b_1 \right) K_0 \left( \sqrt{x_2 x'_2} Q b_2 \right), \quad (3)$$

$$\hat{T}_2 = \frac{8}{3} C_F \alpha_s(t_{21}) \alpha_s(t_{22}) K_0 \left( \sqrt{x_1 x'_1} Q b_1 \right) K_0 \left( \sqrt{x_2 x'_2} Q b_2 \right), \quad (4)$$

where the  $K_0$  are modified Bessel functions of order 0 and  $b_l$  denotes the length of the corresponding transverse-distance vector.

The renormalization scale is chosen in such a way that each hard gluon refers to its own individual momentum scale  $t_{ji}$  to be used in the argument of the corresponding  $\alpha_s$ . The  $t_{ji}$  is defined as the maximum scale of either the longitudinal momentum or the inverse transverse separation, associated with each of the gluons: viz.

$$\begin{aligned} t_{11} &= \max \left[ \sqrt{(1-x_1)(1-x'_1)} Q, 1/b_1 \right], \\ t_{21} &= \max \left[ \sqrt{x_1 x'_1} Q, 1/b_1 \right], \\ t_{12} &= t_{22} = \max \left[ \sqrt{x_2 x'_2} Q, 1/b_2 \right]. \end{aligned} \quad (5)$$

Since the hard scattering amplitudes depend only on the differences of initial and final state transverse momenta, there are only two transverse separation vectors, namely those between quarks 1 and 3 and between quarks 2 and 3:  $\vec{b}_1 (= \vec{b}'_1)$ ,  $\vec{b}_2 (= \vec{b}'_2)$ . Accordingly, the transverse separation between quark 1 and quark 2 is  $\vec{b}_3 = \vec{b}_2 - \vec{b}_1$ .

The soft part of the form factor is given by the following expressions which contain linear combinations of products of the initial and final state wave functions in the transverse configuration space, weighted by  $x_i$ -dependent factors arising from the fermion propagators:

$$\hat{Y}_1^n = \frac{1}{(1-x_1)(1-x'_1)} \left\{ -2\hat{\Psi}_{123}^{*\prime} \hat{\Psi}_{123} - 2\hat{\Psi}_{132}^{*\prime} \hat{\Psi}_{132} + \hat{\Psi}_{231}^{*\prime} \hat{\Psi}_{231} + \hat{\Psi}_{321}^{*\prime} \hat{\Psi}_{321} \right. \\ \left. - \hat{\Psi}_{231}^{*\prime} \hat{\Psi}_{132} - \hat{\Psi}_{132}^{*\prime} \hat{\Psi}_{231} - \hat{\Psi}_{321}^{*\prime} \hat{\Psi}_{123} - \hat{\Psi}_{123}^{*\prime} \hat{\Psi}_{321} \right\} \quad (6)$$

$$\hat{Y}_2^n = \frac{1}{(1-x_2)(1-x'_1)} \left\{ \hat{\Psi}_{231}^{*\prime} \hat{\Psi}_{231} + \hat{\Psi}_{231}^{*\prime} \hat{\Psi}_{132} + \hat{\Psi}_{132}^{*\prime} \hat{\Psi}_{231} \right\} \\ + \frac{1}{(1-x_3)(1-x'_1)} \left\{ 2\hat{\Psi}_{321}^{*\prime} \hat{\Psi}_{321} - \hat{\Psi}_{123}^{*\prime} \hat{\Psi}_{123} + \hat{\Psi}_{321}^{*\prime} \hat{\Psi}_{123} + \hat{\Psi}_{123}^{*\prime} \hat{\Psi}_{321} \right\}. \quad (7)$$

The Fourier transform of the wave function reads

$$\hat{\Psi}_{123}(x, \vec{b}, \mu_F) = \frac{1}{8\sqrt{N_c!}} f_N(\mu_F) \Phi_{123}(x, \mu_F) \hat{\Omega}_{123}(x, \vec{b}), \quad (8)$$

wherein its intrinsic  $k_\perp$ -dependence is parametrized according to the Gaussian

$$\hat{\Omega}_{123}(x, \vec{b}) = (4\pi)^2 \exp \left\{ -\frac{1}{4a^2} [x_1 x_3 b_1^2 + x_2 x_3 b_2^2 + x_1 x_2 b_3^2] \right\}. \quad (9)$$

We have used the convenient short-hand notation  $\hat{\Psi}_{123}(x, \vec{b}) = \hat{\Psi}(x_1, \vec{b}; x_2, \vec{b}; x_3, \vec{b})$  denoting in  $\Phi_{123}(x, \mu_F)$  the factorization scale of short-and large-distance contributions by  $\mu_F$ .

The exponentials  $e^{-S_j}$  in (2) are the Sudakov factors responsible for the effects of gluonic radiative corrections. They have been calculated by Botts and Sterman [3] using resummation techniques in the context of the renormalization group (RG) and having recourse to previous extensive work by Collins, Soper, and Sterman [18]. The explicit expressions for the Sudakov exponents are given in [2,5].

The analytical and numerical evaluation of the neutron form factor is performed under the imposition of the ‘‘MAX’’ IR-prescription [1] on the Sudakov factor, i.e., setting

$$\tilde{b} \equiv \max\{b_1, b_2, b_3\} = \tilde{b}_1 = \tilde{b}_2 = \tilde{b}_3. \quad (10)$$

The results of this calculation are typified by the curves shown in Fig. 1 for the COZ DA [14] (solid line), including also the intrinsic transverse momentum in two different ways: (i) by normalizing the probability  $P_{3q}$  for finding three valence quarks in the neutron to unity (dashed line), which results to  $\langle k_\perp^2 \rangle^{1/2} = 271$  MeV; and (ii) by setting the value of the r.m.s. transverse momentum equal to 600 MeV (dotted line), which implies  $P_{3q} = 0.042$ . Here

and below we throughout use the values  $\Lambda_{\text{QCD}} = 180 \text{ MeV}$  and  $|f_N| = (5.0 \pm 0.3) \times 10^{-3} \text{ GeV}^2$  [14], the latter being the value of the nucleon DA at the origin. The momentum evolution of the DA is RG-controlled—provided the model DA is satisfying the nucleon evolution equation [4], which is true for all DAs we consider in this work. Then the nucleon DA can be expanded in terms of the eigenfunctions of the one-gluon exchange kernel to read

$$\Phi_{123}(x, \mu) = \Phi_{123}^{\text{as}}(x) \sum_n B_n \left( \frac{\alpha_s(\mu)}{\alpha_s(\mu_0)} \right)^{\tilde{\gamma}_n/\beta_0} \tilde{\Phi}_{123}^n(x), \quad (11)$$

where the notations of [16] are adopted and  $\Phi_{123}^{\text{as}}(x) = 120x_1x_2x_3$  is the asymptotic DA. The exponents  $\tilde{\gamma}_n$  are related to the anomalous dimensions of trilinear quark operators with isospin 1/2 (see [19]) and resemble the  $b_n$  in the Brodsky-Lepage notation [4]. Because they are positive fractional numbers increasing with  $n$ , higher-order terms in (11) are gradually suppressed. The constants  $\tilde{\gamma}_n$  are given in [1,5];  $\beta_0 = 11 - 2n_f/3 = 9$  for three flavors. Under these conditions we may use QCD sum-rule results on the moments

$$\Phi^{(n_1 n_2 n_3)}(\mu_0) = \int_0^1 [dx] x_1^{n_1} x_2^{n_2} x_3^{n_3} \Phi_{123}(x, \mu_0) \quad (12)$$

to constrain the first few expansion coefficients  $B_n$  (for more details see [13,16,17]).

As can be seen from Fig. 1 and comparison with [17], the magnitude of the neutron magnetic form factor with Sudakov correction is reduced by more than a factor of 2.5 with respect to the standard HSP. This reduction is enhanced when the intrinsic transverse momentum is included and is pertinent to all nucleon DAs [12,13] modelled on the basis of existing QCD sum-rules [14,15] (shaded band in Fig. 2). The upper region of the band is characterized by COZ-like [14] DAs, whereas its lower part is associated with the recently proposed “heterotic” DA [20]. We note that the perturbative contribution becomes self-consistent for momentum transfers larger than  $8 \text{ GeV}^2$  (using  $\langle k_{\perp}^2 \rangle^{1/2} = 271 \text{ MeV}$ ) in the sense that at least 50 % of the result is accumulated in regions where  $\alpha_s^2$  is smaller than 0.5.

It is important to emphasize that the neutron magnetic form factor is the first process calculated within the modified HSP that yields predictions which indicate overlap with the existing data [21], as can be seen from Fig. 2. This tentative agreement occurs at data

points corresponding to the largest momentum transfers measured, where, incidentally, our theoretical calculations become self-consistent. Therefore, measurements of the neutron magnetic form factor beyond  $10 \text{ GeV}^2$  are extremely important in order to check the validity of the theoretical predictions in a more quantitative way.

One place to test these results is in the data for the differential cross sections for elastic electron-proton and electron-neutron scattering  $\sigma_p$  and  $\sigma_n$ , respectively. For small scattering angles, where the terms  $\propto \tan^2(\theta/2)$  can be neglected, and for large  $Q^2$ , the ratio  $\sigma_n/\sigma_p$  becomes in a slightly model-dependent way proportional to the square of the ratio of the neutron to the proton magnetic form factor.

Combining our calculations for the proton [1] with those presented here for the neutron, we can extract theoretical predictions for  $\sigma_n/\sigma_p$  by inputting the same set of model DAs for the nucleon [12,13] as before. The results are shown in Fig. 3 (shaded area) in comparison with available data [22]. From this figure we see that the measured values of  $\sigma_n/\sigma_p$  enter the estimated range already at  $Q^2 \approx 8 \text{ GeV}^2$ . [The corresponding values of the ratio  $-G_M^n/G_M^p$ , allowed by our analysis, range between -0.2 and 0.5.] The fair agreement between theoretical predictions and data is partly deceptive owing to the fact that the self-consistent calculation of the leading-order perturbative contribution to the proton magnetic form factor within the modified HSP yields a rather small value [1]. This missing part of the proton form factor can arise from many sources, e.g, from a large K-factor and/or higher-twist contributions and would certainly affect the width of the strip. Such contributions are also conceivable for the neutron form factor.

In any case it is remarkable that the collective pattern of solutions to the QCD sum rules [14,15], found within the standard HSP [12,13], pertains to the inclusion of transverse-momentum contributions comprising the Sudakov factor and those due to the intrinsic transverse momentum (see Fig. 4). Indeed, the solutions arrange themselves across an “orbit” in the  $(B_4, -G_M^n/G_M^p)$  plane which is somewhat shifted compared to the original one. In contrast to the standard HSP version, within the present context, the “orbit” is slightly  $Q^2$ -dependent, as shown in Fig. 4. The new “orbit” at  $Q^2 = 30 \text{ GeV}^2$  can be characterized

by the empirical relation  $-G_M^n/G_M^p = 0.426 - 9.91 \times 10^{-3} B_4 - 4.27 \times 10^{-4} B_4^2 + 4.59 \times 10^{-6} B_4^3$ , which complies with that found in [12]. The dashed line in Fig. 4 represents a similar fit for  $Q^2 = 10^3 \text{ GeV}^2$ . We observe that with increasing momentum transfer, the “orbit” within the modified HSP transmutes into that of the standard HSP. We note that the coefficient  $B_4$  projects onto the eigenfunction  $\tilde{\Phi}_4(x_i)$  and hence provides an effective measure to account for the antisymmetric content of the nucleon DA, since the other antisymmetric eigenfunctions are offset by this term [12].

In summary, in this letter the modified HSP has been applied to the neutron magnetic form factor for the first time. In contrast to other cases (e.g., pion and proton electromagnetic form factors), the band of predictions obtained with the set of model DAs for the nucleon indicates overlap with the experimental data at the largest measured values of momentum transfer, where the theoretical predictions become self-consistent. Nevertheless, it is likely that in order to improve agreement with the data, several additional contributions have to be included: Perturbative higher-order corrections may give rise to a rather large K-factor of the order of 2 multiplying the leading-order contribution, as found for other large-momentum transfer processes [23]. However, for the case of the pion form factor, already existing calculations [24,25] of the K-factor to one-loop order indicate that with an appropriate choice of the renormalization point, the actual value of the K-factor is rather small, i.e., of order unity. On the other hand, still unestimated contributions due to higher twists are presumably sizeable in the experimentally accessible region and may also be important.

## ACKNOWLEDGMENTS

This work was supported in part by the Deutsche Forschungsgemeinschaft and the Bundesministerium für Forschung und Technologie FRG under contract 06WU737.

## REFERENCES

- [1] J. Bolz, R. Jakob, P. Kroll, M. Bergmann, and N.G. Stefanis, Wuppertal preprint WU-B-94-06 and Bochum preprint RUB-TPII-94-01 (May 1994), submitted to Z. Phys. C - Particles and Fields.
- [2] H.-N. Li and G. Sterman, Nucl. Phys. B 381 (1992) 129.
- [3] J. Botts and G. Sterman, Nucl. Phys. B 325 (1989) 62.
- [4] G.P. Lepage and S.J. Brodsky, Phys. Rev. D 22 (1980) 2157.
- [5] H.-N. Li, Phys. Rev. D 48 (1993) 4243.
- [6] T. Hyer, Phys. Rev. D 47 (1993) 3875.
- [7] M.G. Sotiropoulos and G. Sterman, Stony Brook Report ITP-SB-93-83 (January 1994).
- [8] R. Jakob and P. Kroll, Phys. Lett. B 315 (1993) 463; B 319 (1993) 545(E).
- [9] P. Kroll, Proceedings of the Workshop on Hadron Structure '93, S. Dubnička and A.Z. Dubničková (Eds.), Banská Štiavnica, Slovakia, Sept. 5-10, 1993.
- [10] R.G. Arnold et al., Phys. Rev. Lett. 57 (1986) 174.
- [11] A.F. Sill et al., Phys. Rev. D 48 (1993) 29.
- [12] M. Bergmann and N.G. Stefanis, Phys. Rev. D 48 (1993) R2990.
- [13] M. Bergmann and N.G. Stefanis, Phys. Lett. B 325 (1994) 183.
- [14] V.L. Chernyak, A.A. Ogloblin, and I.R. Zhitnitsky, Z. Phys. C 42 (1989) 569.
- [15] I.D. King and C.T. Sachrajda, Nucl. Phys. B 279 (1987) 785.
- [16] N.G. Stefanis, Phys. Rev. D 40 (1989) 2305; D 44 (1991) 1616(E)
- [17] N.G. Stefanis and M. Bergmann, Proceedings of the Workshop on Exclusive Reactions at High Momentum Transfer, C.E. Carlson, P. Stoler, and M. Taiuti (Eds.), Elba, Italy,

24-26 June, 1993, World Scientific, Singapore, 1994; Proceedings of the Workshop on Hadron Structure '93, S. Dubnička and A.Z. Dubničková (Eds.), Banská Štiavnica, Slovakia, Sept. 5-10, 1993; Proceedings of the Workshop on Quantum Field Theoretical Aspects of High Energy Physics, B. Geyer and E.-M. Ilgenfritz (Eds.), Kyffhäuser, Germany, Sept. 20-24, 1993.

- [18] J.C. Collins and D.E. Soper, Nucl. Phys. B 193 (1981) 381; B 194 (1982) 445; J.C. Collins, D.E. Soper, and G. Sterman, Nucl. Phys. B 261 (1985) 104.
- [19] M. Peskin, Phys. Lett. 88 B (1979) 128.
- [20] N.G. Stefanis and M. Bergmann, Phys. Rev. D 47 (1993) R3685.
- [21] P. Bosted et al., Phys. Rev. Lett. 68 (1992) 3841; S. Platchkov et al., Nucl. Phys. A 510 (1990) 740.
- [22] S. Rock et al., Phys. Rev. D 46 (1992) 24.
- [23] N.G. Antoniou et al., Phys. Lett. B 128 (1983) 257.
- [24] R.D. Field et al., Nucl. Phys. B 186 (1981) 429.
- [25] F.M. Dittes and A.V. Radyushkin, Yad. Fiz. 34 (1981) 529 [Sov. J. Nucl. Phys. 34 (1981) 293].

## FIGURES

FIG. 1. The influence of the intrinsic transverse momentum on the neutron magnetic form factor within the modified HSP. The curves shown are obtained for the COZ [14] DA by imposing the “MAX” prescription including evolution. The solid line represents the results without  $k_{\perp}$ -dependence, whereas the dashed and dotted lines are obtained with  $\langle k_{\perp}^2 \rangle^{1/2} = 271$  MeV and 600 MeV, respectively.

FIG. 2. The neutron magnetic form factor vs.  $Q^2$ . The theoretical results are obtained using the “MAX” prescription including evolution and normalizing the wave functions to unity. The shadowed strip indicates the range of predictions derived from the set of DAs determined in [12] in the context of QCD sum rules (see text). The solid (dashed, dotted) line corresponds to the COZ (heterotic, optimized COZ) DA (cf. Fig. 4). The data are taken from [21].

FIG. 3. The ratio  $\sigma_n^{el}/\sigma_p^{el}$  of the differential elastic electron-neutron to electron-proton cross section vs.  $Q^2$  at scattering angles of  $10^\circ$ . The shaded area and model DAs for the nucleon correspond to those shown in Fig. 2. The data are taken from [22].

FIG. 4. Relation between the ratio  $R$  of the magnetic nucleon form factors and the expansion coefficient  $B_4$  of the Appell polynomial decomposition of the nucleon DA, including the effect of the Sudakov factor. The results are obtained at  $Q^2 = 30$  GeV<sup>2</sup>, employing the “MAX” prescription. The superimposed solid line is an empirical polynomial fit similar to the original one given in [12]. The dashed line serves to illustrate the dependence on the momentum scale ( $Q^2 = 10^3$  GeV<sup>2</sup>).

This figure "fig1-1.png" is available in "png" format from:

<http://arxiv.org/ps/hep-ph/9407250v2>

This figure "fig1-2.png" is available in "png" format from:

<http://arxiv.org/ps/hep-ph/9407250v2>

This figure "fig1-3.png" is available in "png" format from:

<http://arxiv.org/ps/hep-ph/9407250v2>

This figure "fig1-4.png" is available in "png" format from:

<http://arxiv.org/ps/hep-ph/9407250v2>

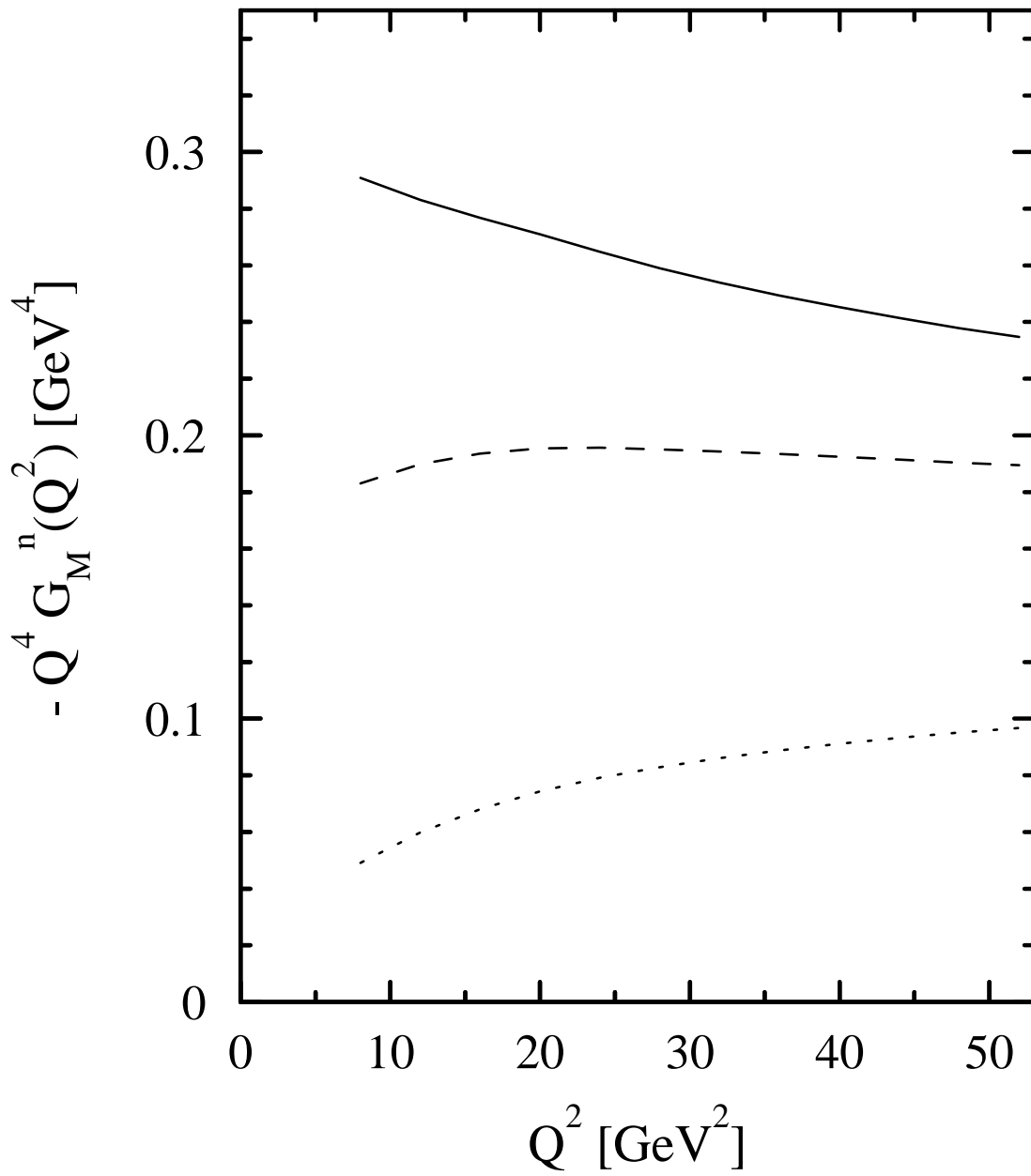


**Figure 1**

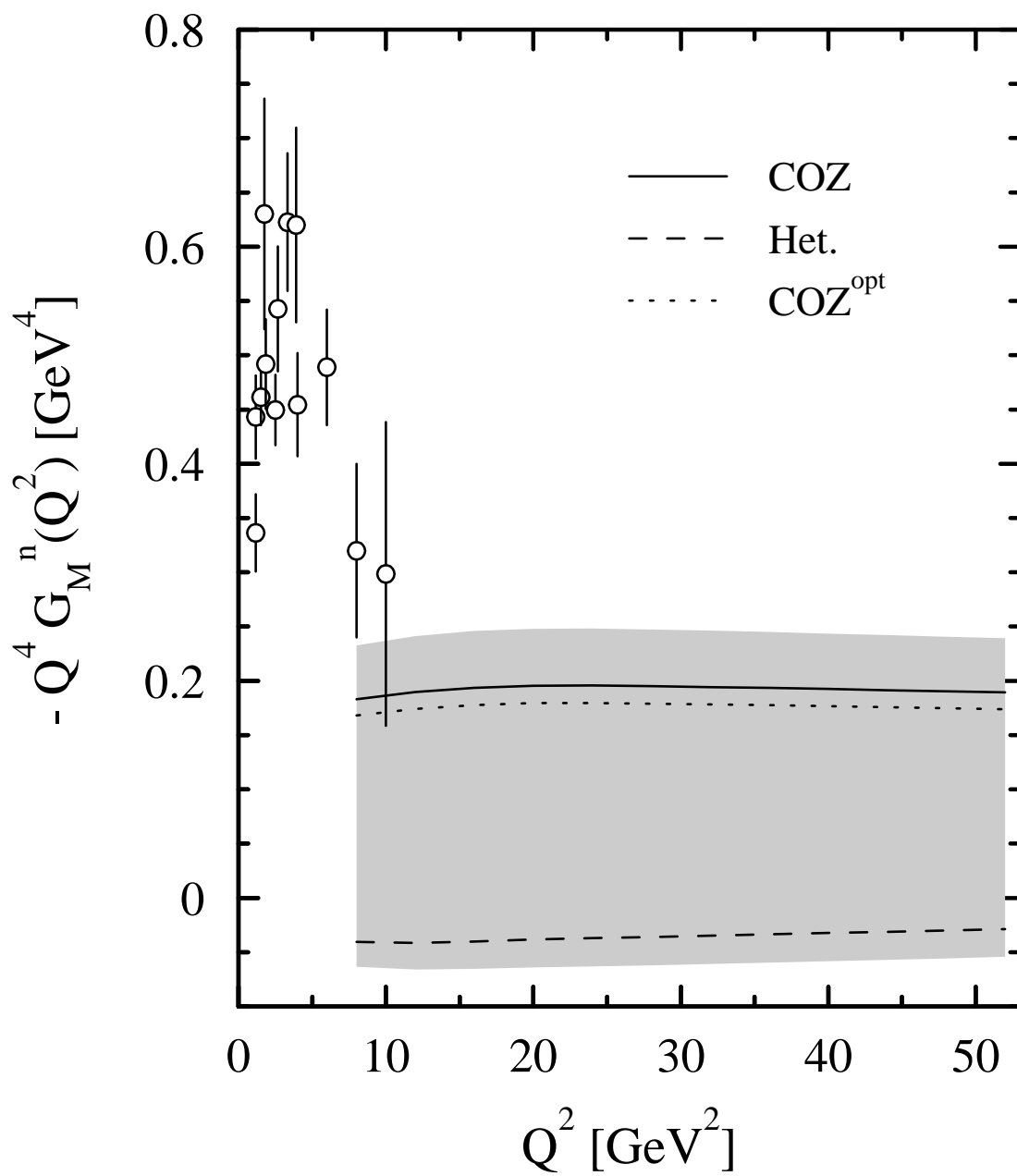


**Figure 2**

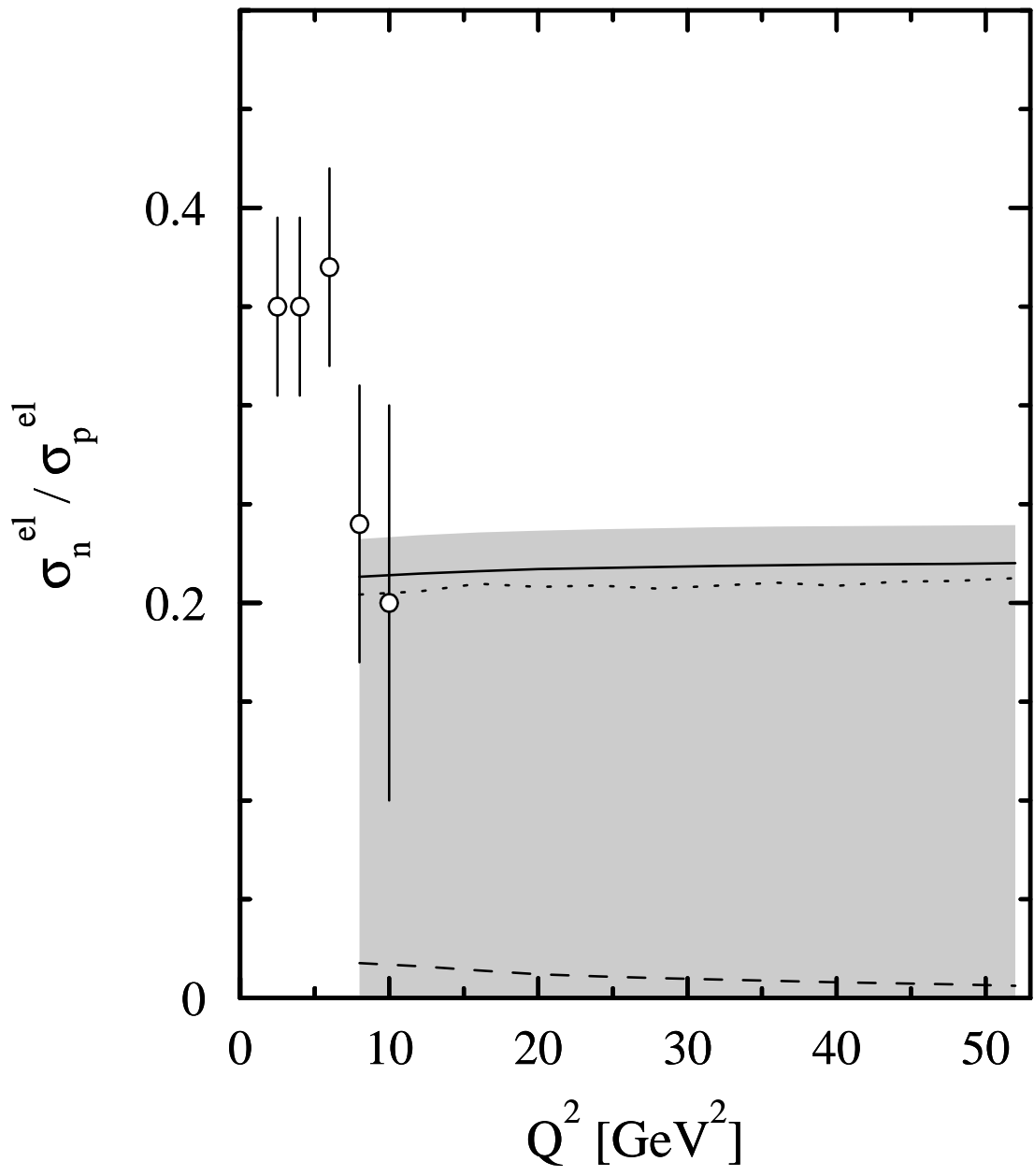


**Figure 3**

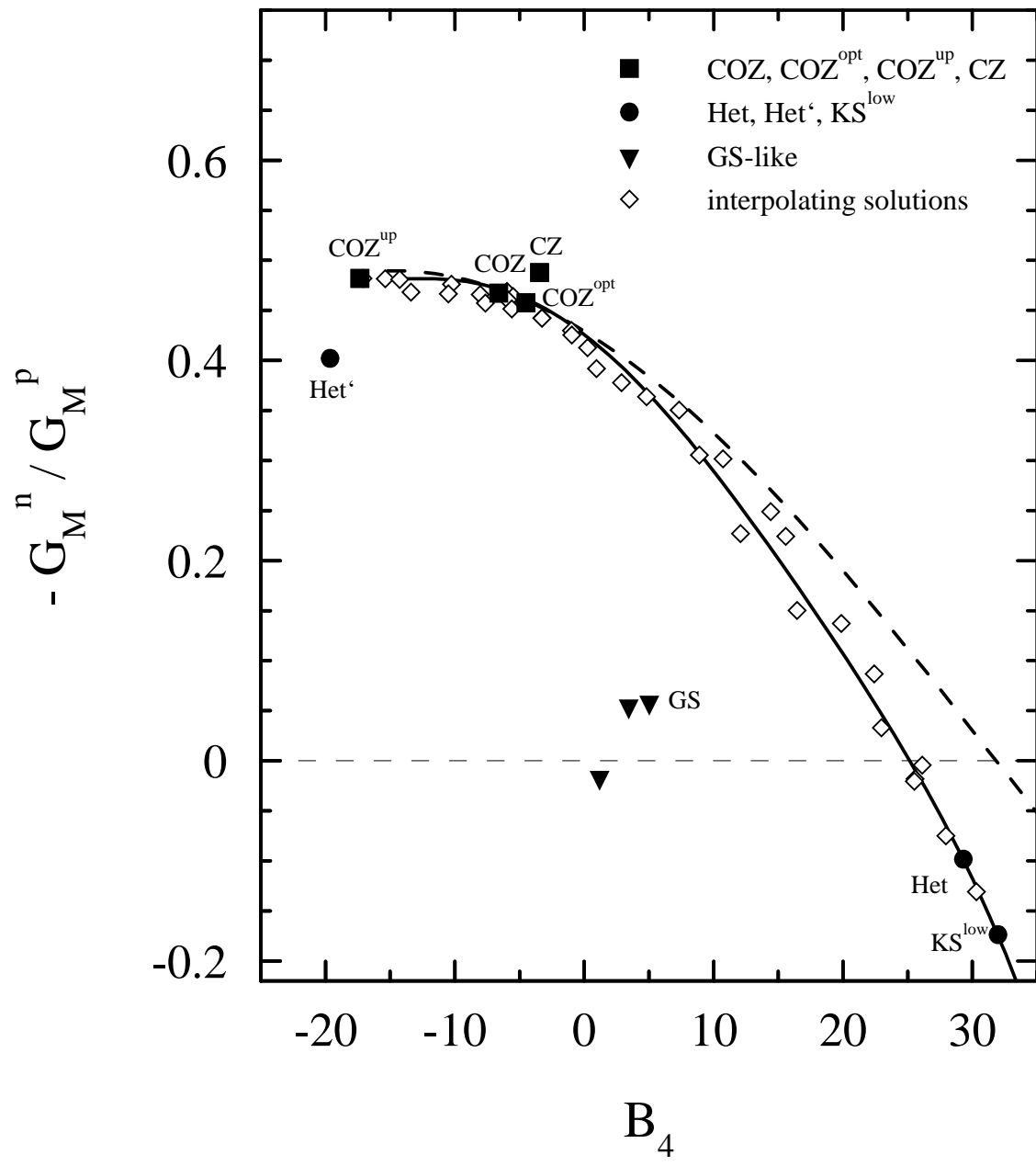


Figure 4